Table S1. Characteristics of the studied glaciers in the Lunana region, Bhutan Himalaya, and summary of the differential GPS surveys in 2004 and 2011. The minimum, medium and maximum elevations and glacier areas are based on ASTER GDEM2 and ALOS PRISM images acquired in 2010 (Nagai et al., 2016). The mean slopes are based on ASTER-DEM. The numbers of survey points are obtained from the 1 m grid DEMs.

Glacier	Elevation			Area	Mean slope	Date of survey		Number of survey points	
	Min	Medium	Max			2004	2011	2004	2011
	(m)	(m)	(m)	(km^2)	(degree)	(MM/DD)	(MM/DD)		
Thorthormi	4283	6163	6872	13.16	0.1	10/02, 03, 05	09/18	25388	25752
Lugge	4561	6000	6847	10.93	11.8	10/06	09/20	8114	17900
Off-glacier						09/29–10/10	09/18–22	38171	64608

Table S2. Details of the ASTER-DEMs used for the elevation change calculation in this study.

Acquisition date (YYYY/MM/DD)	ASTER granule ID
2004/10/11	ASTB041011044607
2011/04/06	ASTB110406044637

Table S3. Dates of the ASTER images used for the surface flow velocity analysis and length of the measurement period.

Pre image (YYYY/MM/DD)	Post image (YYYY/MM/DD)	Length of measurement period (Day (year))
2002/10/22	2003/07/21	273 (0.75)
2006/02/03	2007/01/30	362 (0.99)
2007/01/30	2008/01/01	337 (0.92)
2008/01/01	2009/12/12	712 (1.95)
2009/12/12	2010/10/12	305 (0.83)

Table S4. Details of the ASTER images used for the thermal resistance calculation in this study.

Acquisition date (YYYY/MM/DD)	ASTER granule ID
2002/10/22	AST3A10210220448051102020056
2003/07/21	AST3A10307210446080407230013
2005/09/28	AST3A10509280446011110140033
2006/02/03	AST3A10602030445411110140028
2006/12/04	AST3A10612040446231110140026
2007/05/06	AST3A10705060441001110140025
2007/10/29	AST3A10710290440431110140023
2010/10/12	AST3A11010120446391110140074

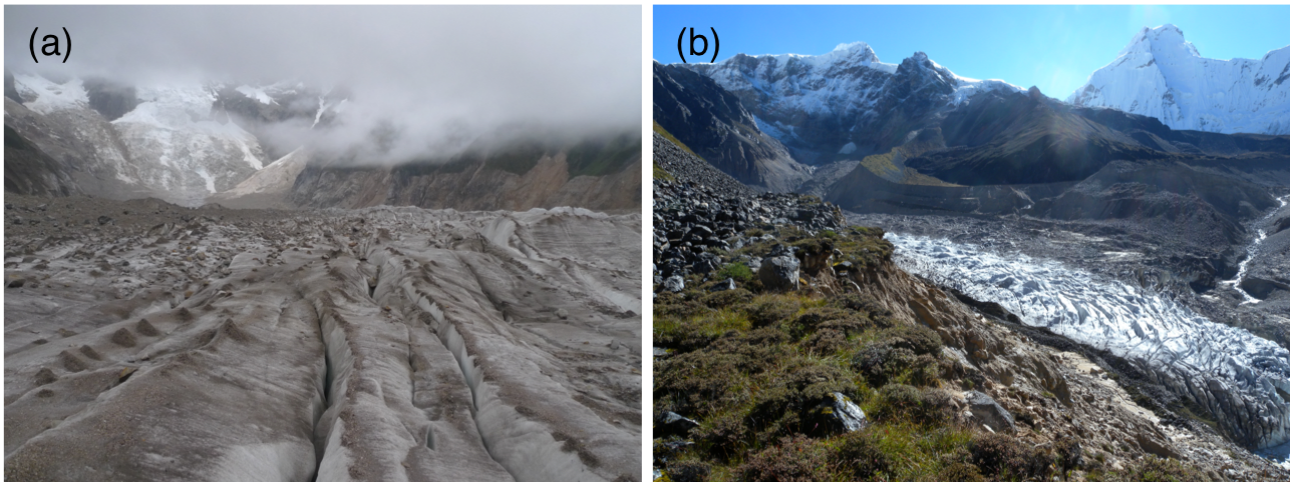

Figure S1. Photographs showing surface condition near the termini of (a) Thorthormi (18 September 2011) and (b) Lugge glaciers (20 September 2011).

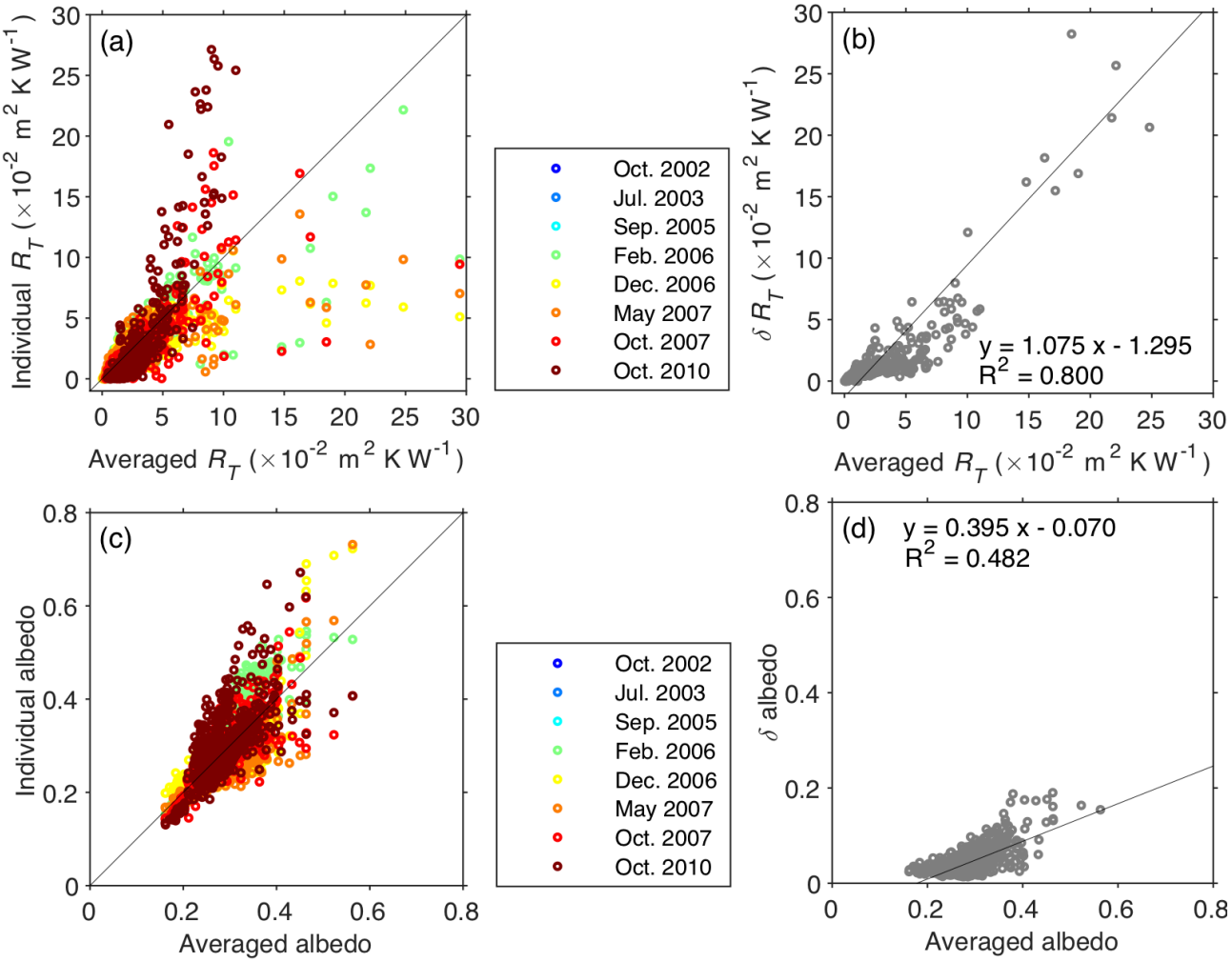

Figure S2. (a) Scattergram and (b) standard deviations (δ) of thermal resistance (R_T), and (c) scattergram and (d) standard deviations of albedo derived from the multitemporal ASTER data against their averages. The mean thermal resistance and albedo were used to calculate surface mass balance.

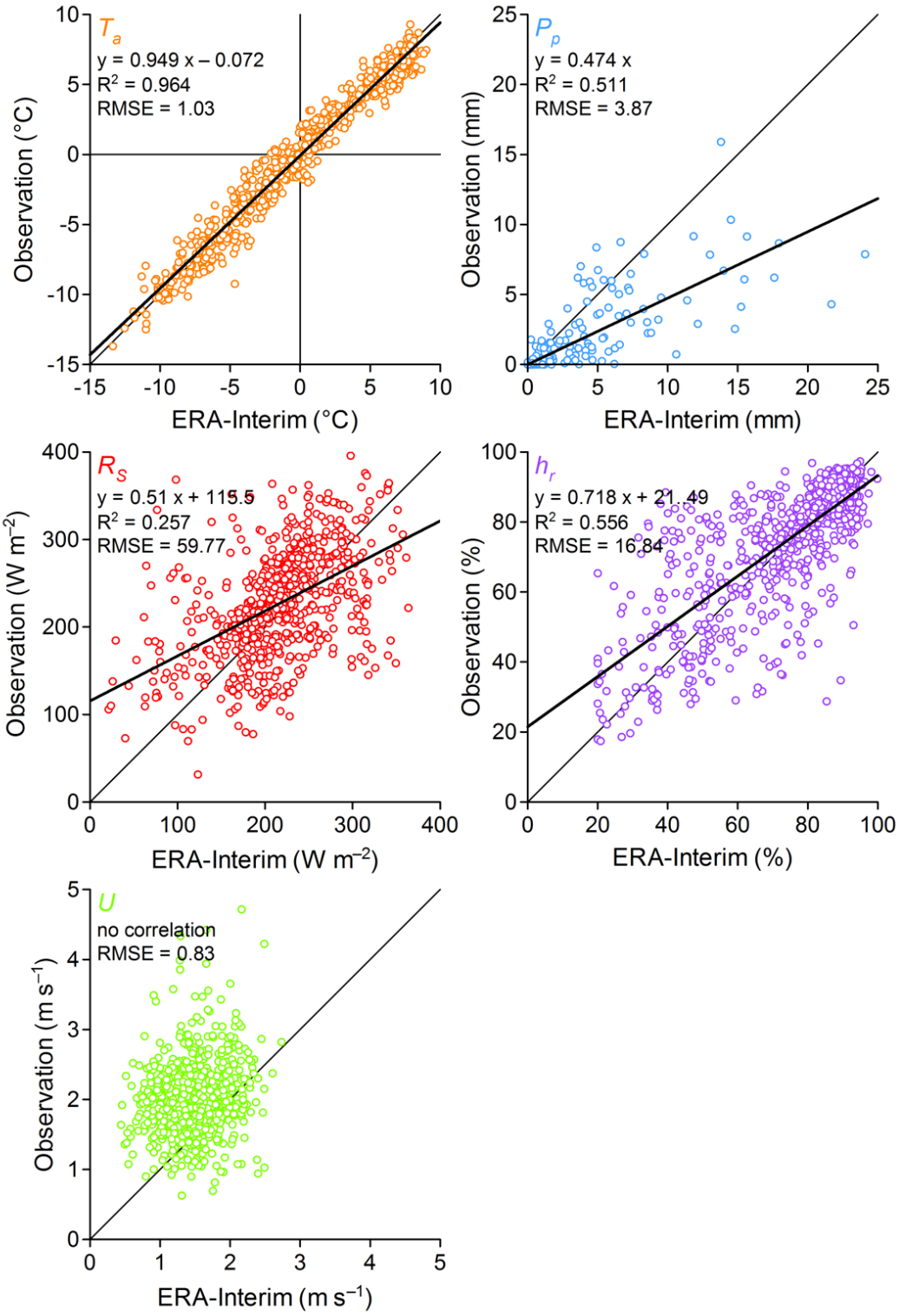

Figure S3. Scatter plot of air temperature (T_a), precipitation (P_p), solar radiation (R_S), relative humidity (h_r), and wind speed (U) between ERA-Interim reanalysis and observational data for 2002–2004.

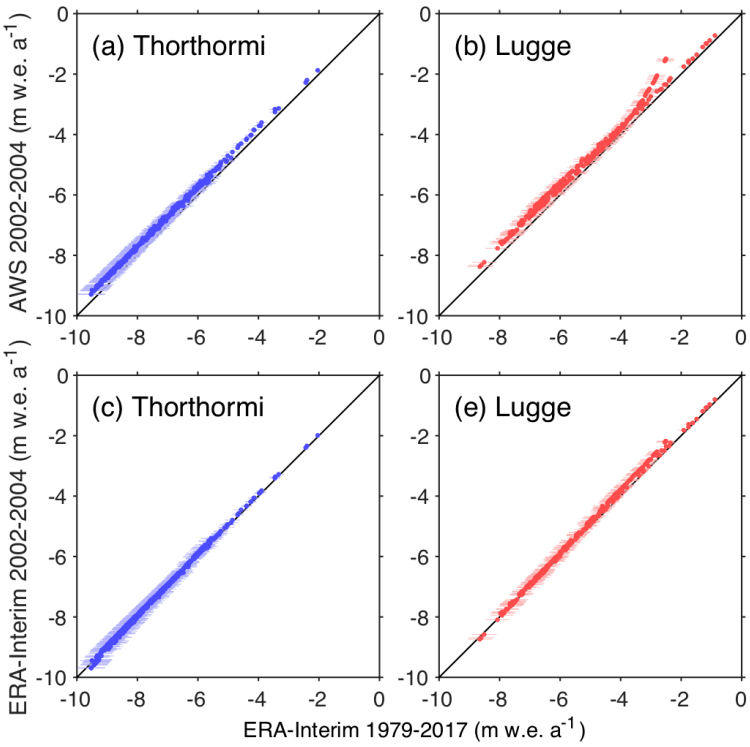

Figure S4. Scatter plot between SMBs of (a and c) Thorthormi and (b and d) Lugge glaciers. SMBs calculated with ERA-Interim reanalysis data (1979–2017) against (a and b) SMBs calculated with observational meteorological data (2002–2004), and (c and d) SMBs calculated with ERA-Interim reanalysis data for the 2002–2004 period.

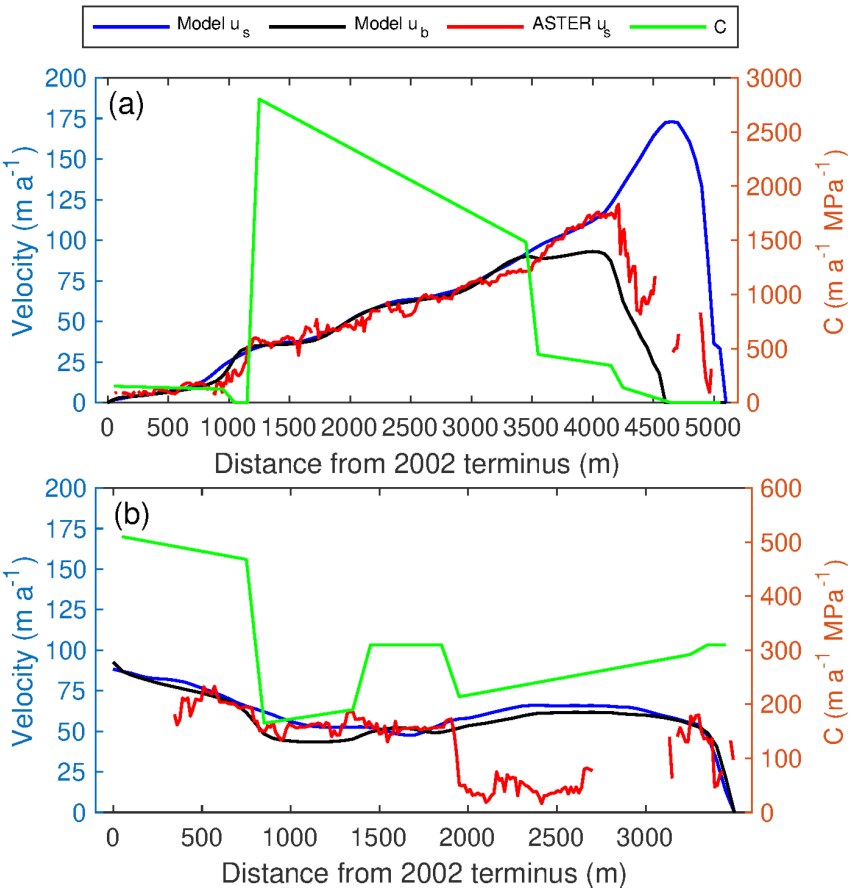

Figure S5. Longitudinal distribution of the sliding coefficient (C) obtained for modelled surface (Model u_s) and basal velocities (Model u_b) to reproduce measured surface velocities (ASTER u_s) for (a) Thorthormi and (b) Lugge glaciers.

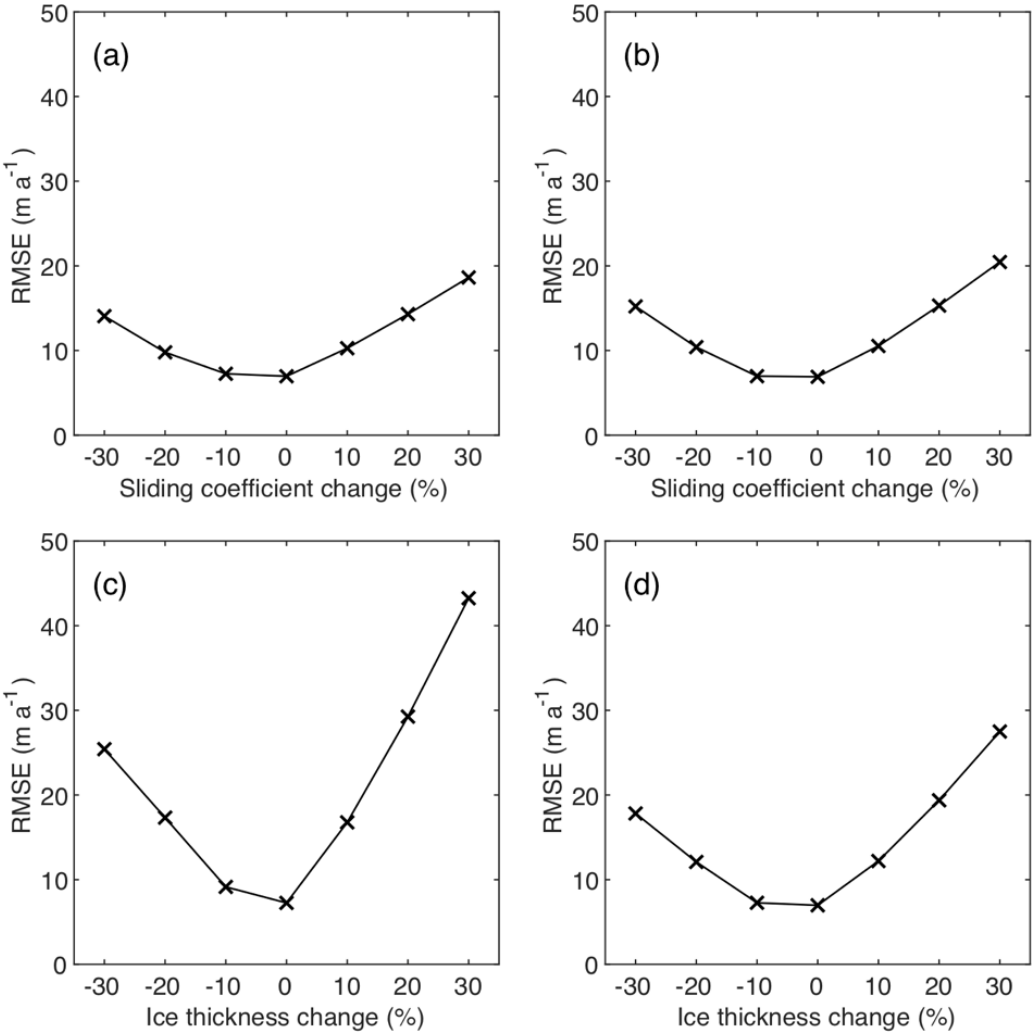

Figure S6. RMSEs between the modelled and measured surface velocities for (a and c) Thorthormi and (b and d) Lugge glaciers, modelled with (a and b) various sliding coefficient (*C*), and (c and d) various ice thickness.

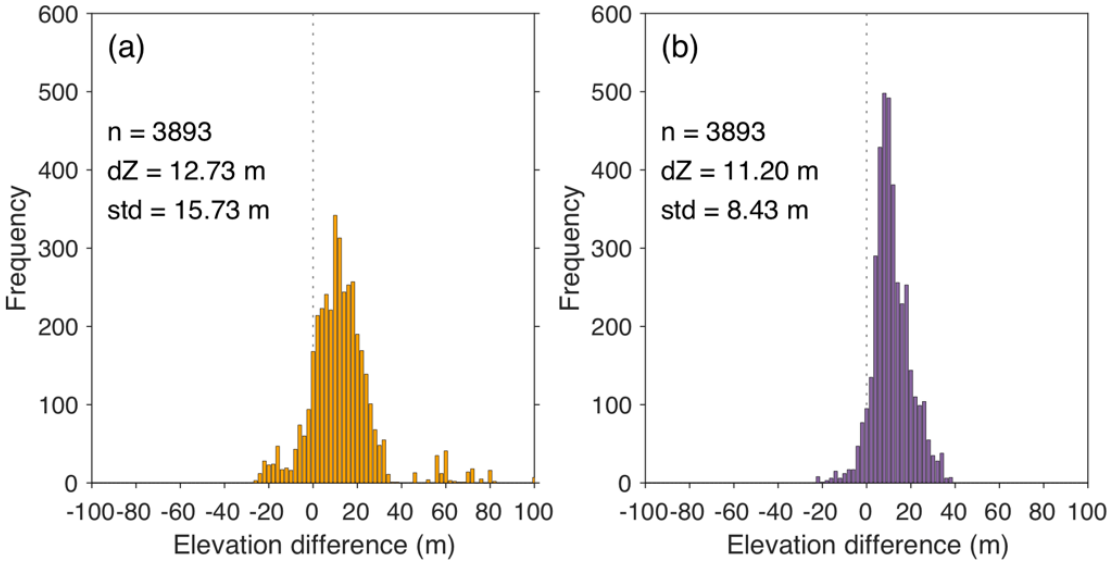

Figure S7. Histogram of the elevation differences from the off-glacier of ASTER-DEMs in (a) 2004 and (b) 2011 against the 2011 DGPS-DEM at 1 m elevation bins.

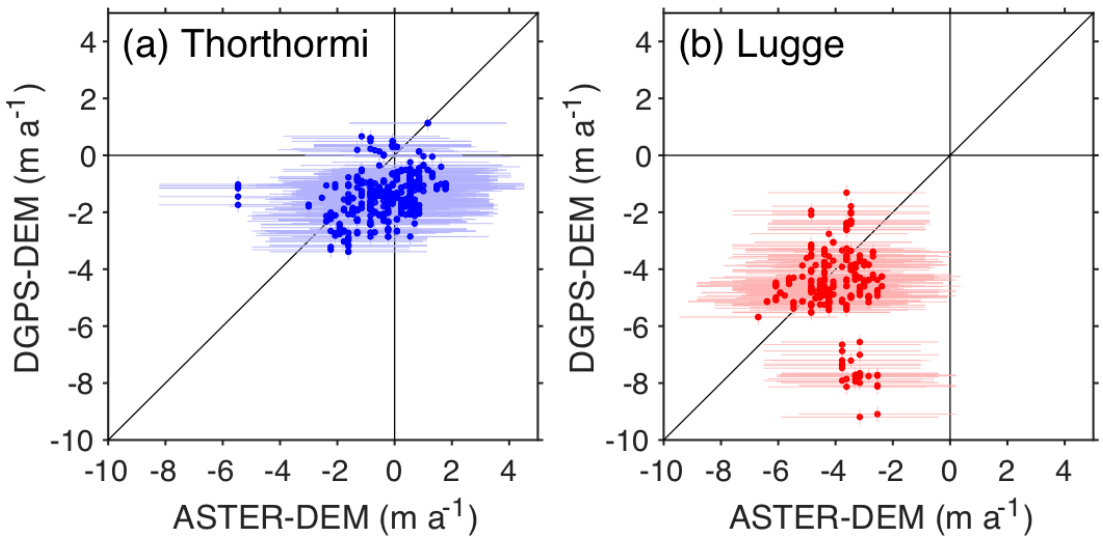

Figure S8. Scatter plot of the rate of surface elevation change between from ASTER-DEMs and DGPS-DEMs at (a) Thorthormi and (b) Lugge glaciers. Error bars denote standard deviations of DEM differences over the ice-free terrain.

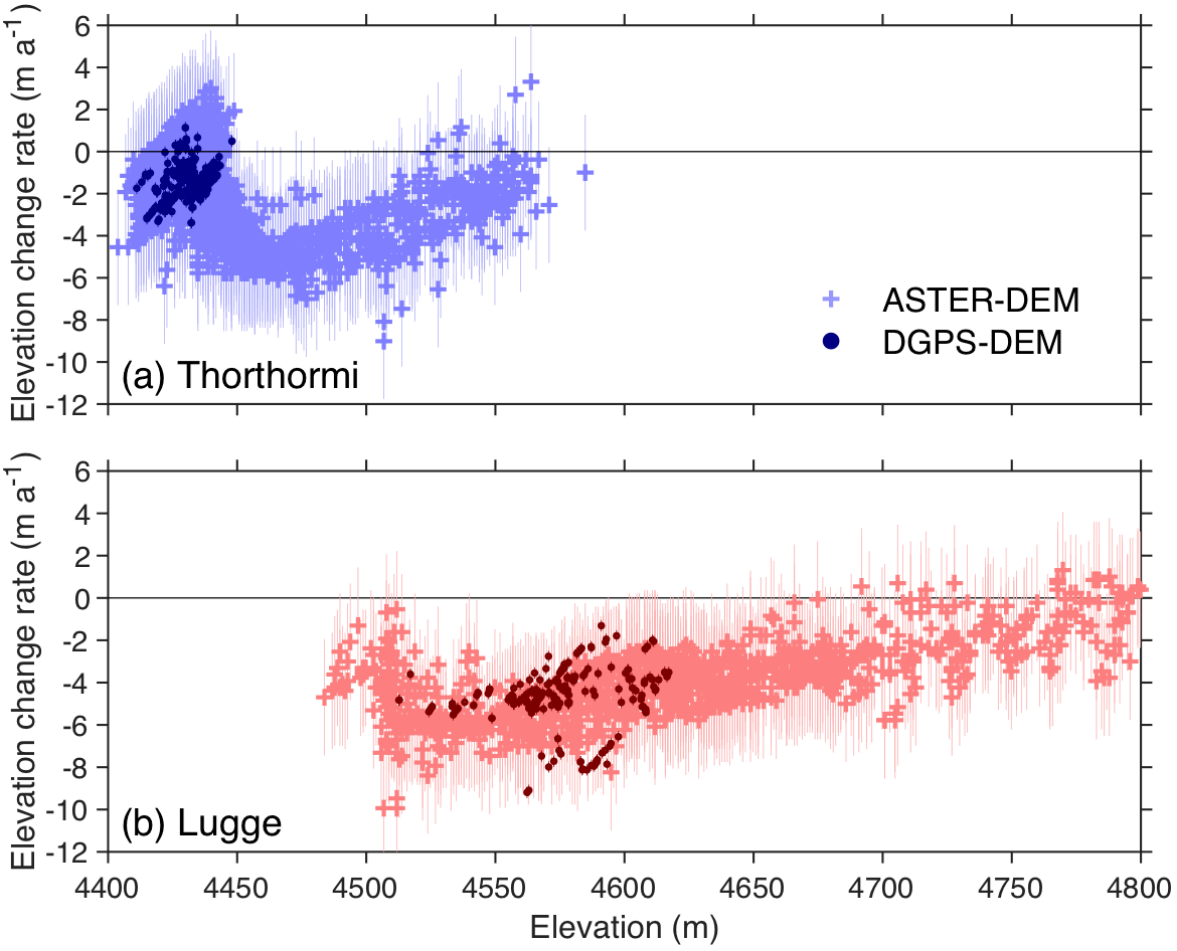

Figure S9. Rate of elevation change along elevation at (a) Thorthormi and (b) Lugge glaciers. Dark-coloured circles are from DGPS-DEMs and light-coloured crosses are from ASTER-DEMs. Error bars denote standard deviations of DEM differences over the ice-free terrain.

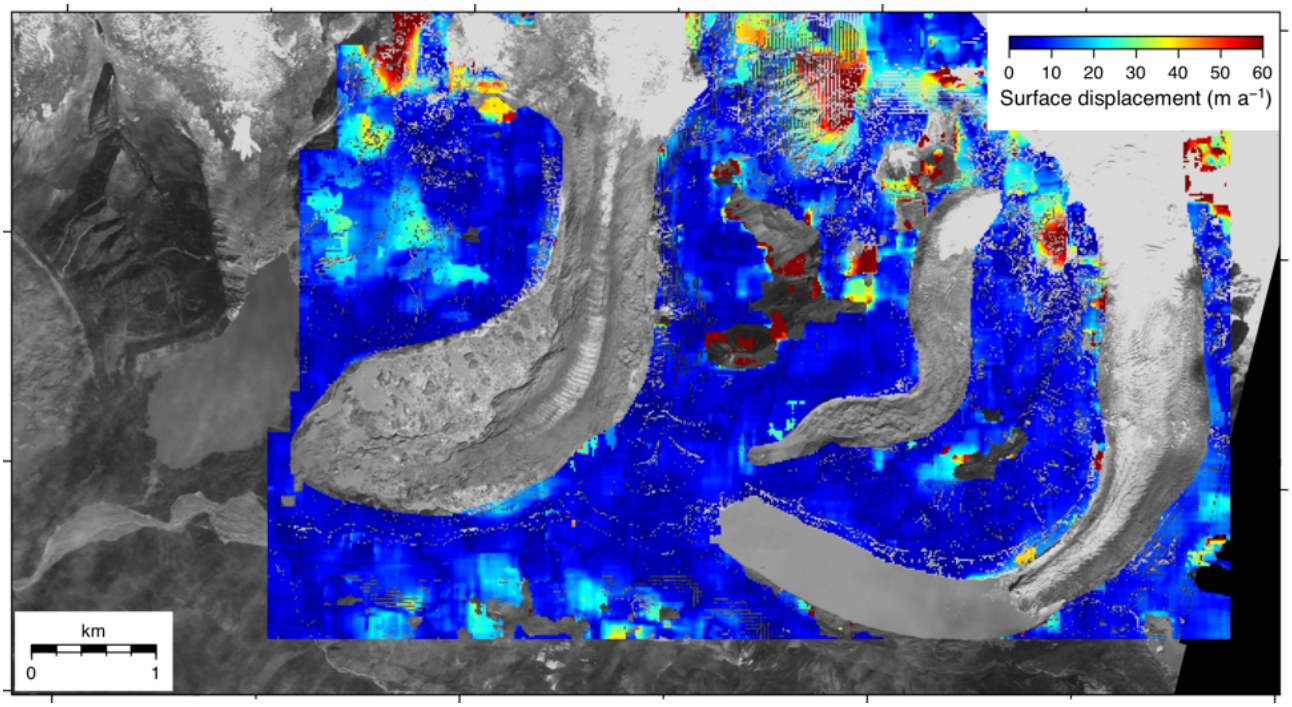

Figure S10. Surface displacements on ice-free terrain derived from image pair on 3 February 2006 and 30 January 2007.

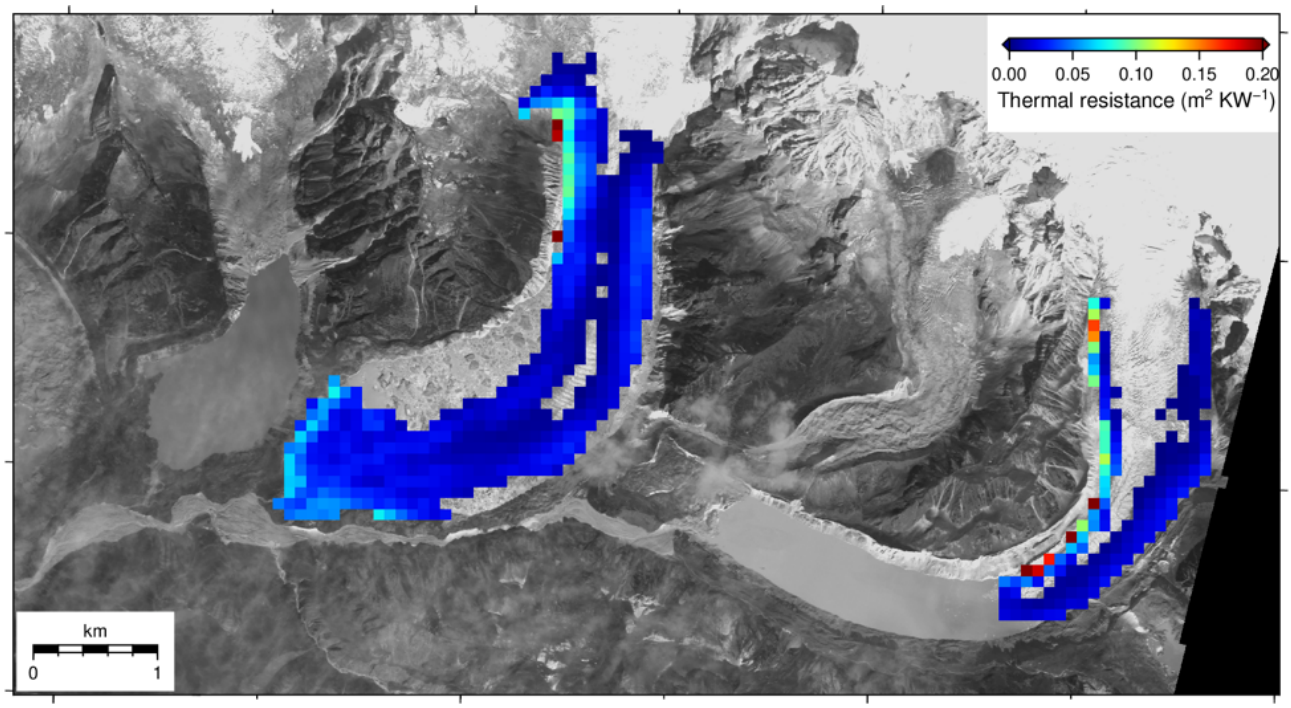

Figure S11. Spatial distribution of thermal resistance used to calculate surface mass balance.

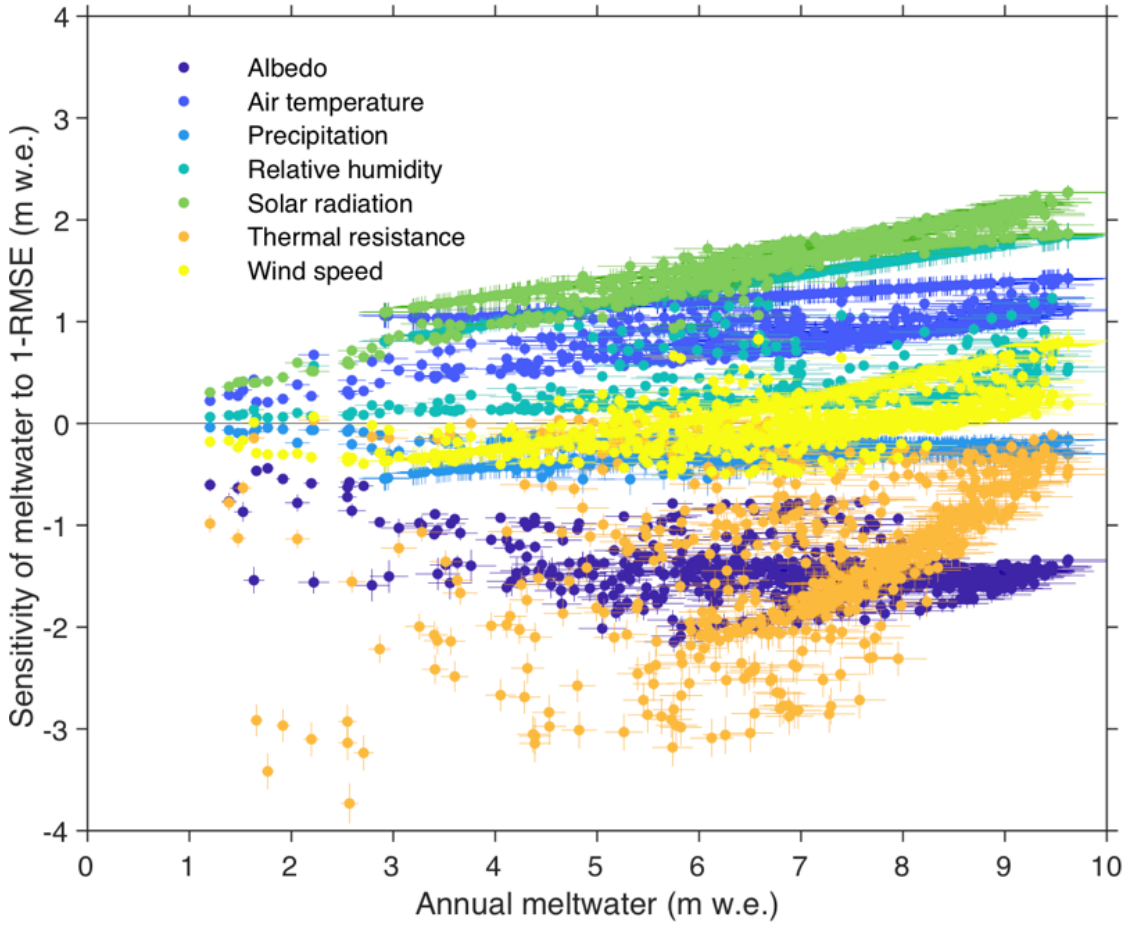

Figure S12. Sensitivity analysis of annual meltwater as a function of RMSE of each meteorological parameter at debris-covered area. Horizontal axis is variable annual meltwater calculated each grid in the SMB model. RMSEs except for albedo and thermal resistance are obtained from ERA-Interim and observed data for 2002–2004 (Fig. S3). Uncertainties of albedo and thermal resistance are derived from 8 satellite images (Fig. S2).

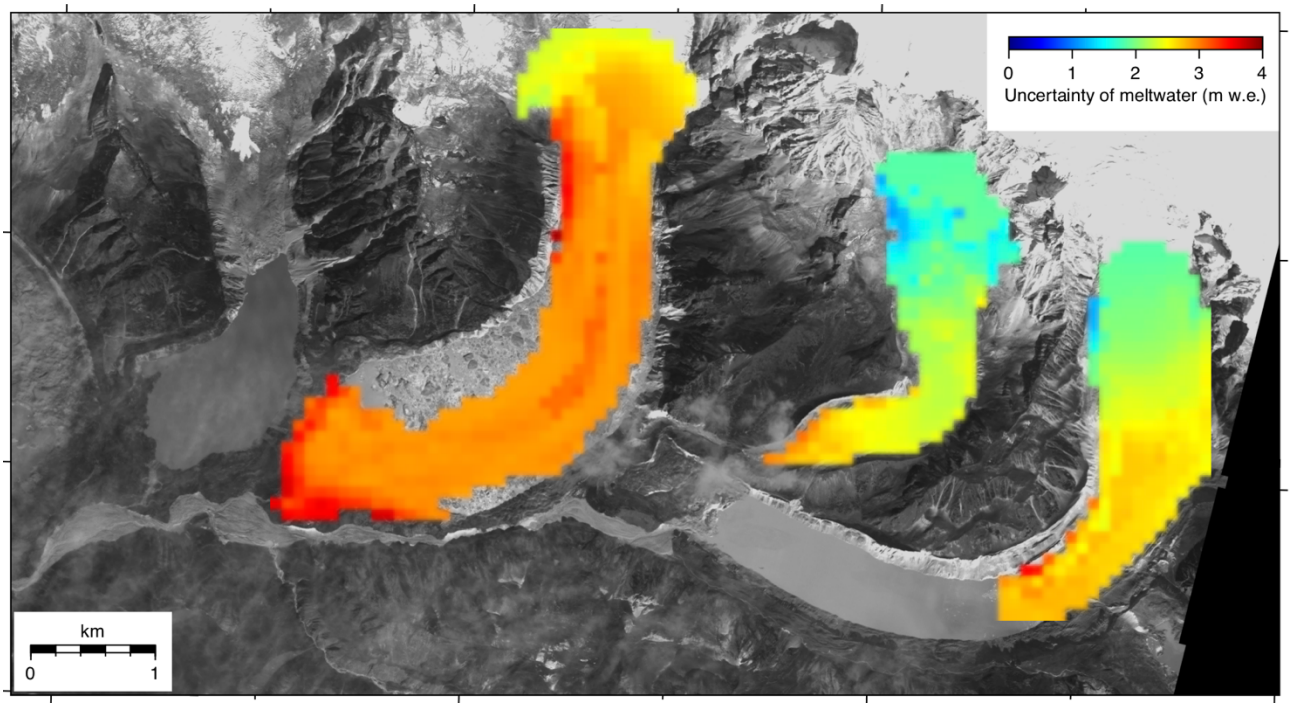

Figure S13. Spatial distribution of estimated meltwater uncertainty.

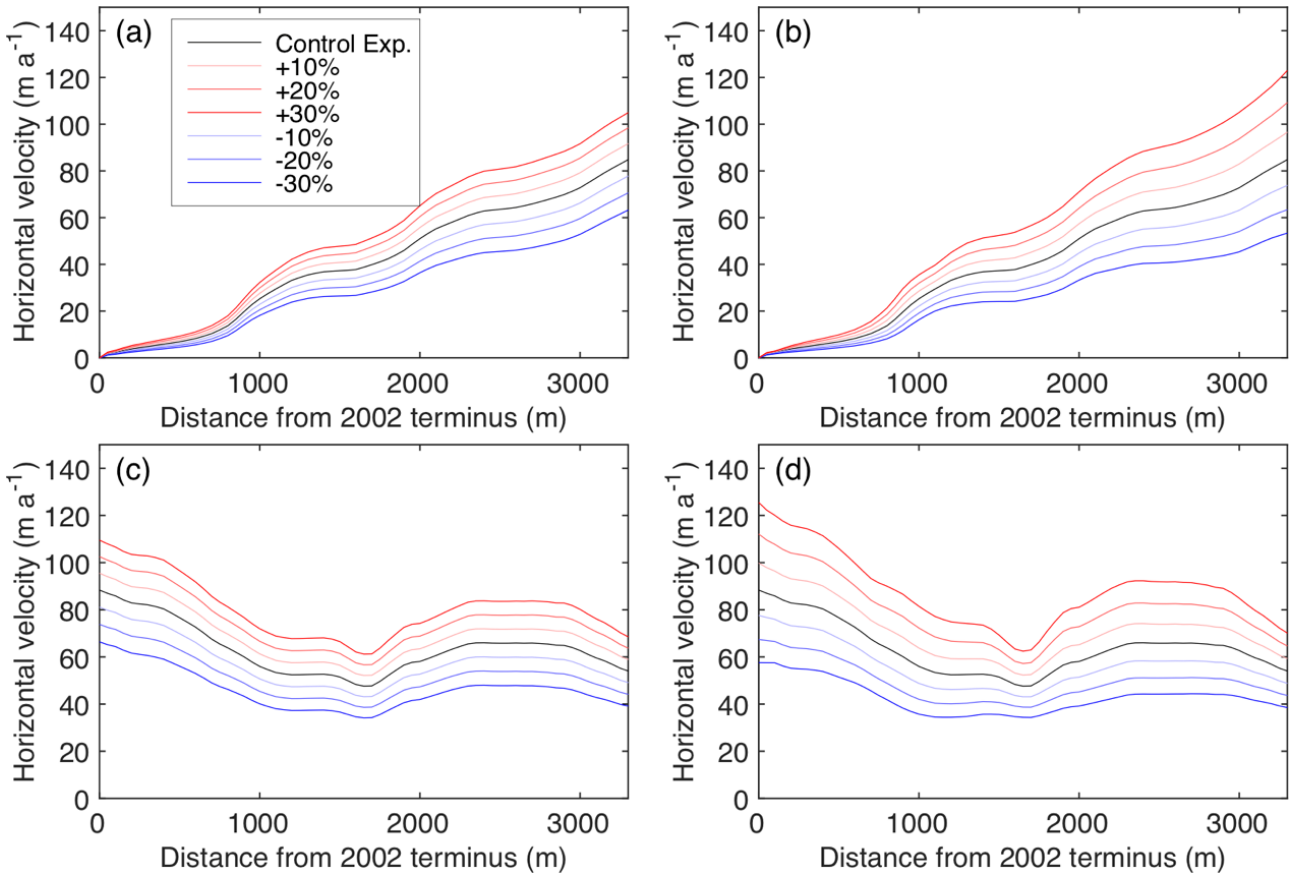

Figure S14. Surface velocity computed for (a and b) Thorthormi and (c and d) Lugge glaciers obtained by changing (a and c) the sliding coefficient (*C*) and (b and d) ice thickness by ±30 %. The black line is the control experiment.